Investigating the Use of Super Conducting Josephson Circuits for Microwave Power Measurements at Cryogenic Temperatures

Tezgül COŞKUN ÖZTÜRK[1], Oliver KIELER[2]

[1]Voltage Laboratory of TÜBİTAK Ulusal Metroloji Enstitüsü (UME) Kocaeli, Turkey
tezgul.ozturk@tubitak.gov.tr
[2]Quantum Electronics of Physikalisch Technische Bundesanstalt (PTB) Braunschweig, Germany
oliver.kieler@ptb.de

Abstract

In this paper, the use of Josephson Arbitrary Waveform Synthesizer System's superconducting integrated circuit consisting of two Josephson Junctions arrays, for microwave power measurements is investigated. The critical current, the temperature dependent phenomena of the Josephson Junctions, is used to compare DC power and MW power reaching the neighbor array. Validation of the method is roughly demonstrated by measuring the attenuation of the waveguide used within the stick used to immerse the circuit to cryogenic environment. The attenuation of the waveguide is measured with the novel sensor and the conventional method. The preliminary results show 0.2 dB consistence of the attenuation measurements between the conventional and the novel method at different power levels at 1 GHz, that suggest that the method can be useful. To improve the repeatability and accuracy by automation, which is essential for such measurements, new power sensor is designed and presented.

1. Introduction

Established AC voltage/current metrology is based on comparing the heat generated by AC quantity with the heat generated by its DC counterpart via AC-DC transfer device which is a resistor in a vacuum and has thermal contact with a temperature sensor [1]. RF power sensor's frequency dependent effective efficiency is calibrated using calorimetric principles and by comparing the heating effect of DC power and RF power onto the sensor [2]. Dry cryocoolers operate under vacuum and need well established thermal contact between the superconducting integrated circuit (SIC) and the cold head of the cooler. The wellness of the thermal conductivity between the SIC and cold head is measured by using critical current of JJs as temperature sensor [3,4]. The possibility of running the Josephson Arbitrary Waveform Synthesizer (JAWS) system in cryocooler is also shown by using one of the arrays of SIC as temperature sensor while the other one is normally operated [5].

Measuring microwave (MW) power at 4 K is challenging and important for increasing needs of cryogenic industry and there is not any established MW power standard yet [6]. TÜBİTAK UME suggested investigating the measurement ability of MW power at 4 K using JAWS arrays by comparing the heat generated by DC power and MW power via critical current measurement of JJs [6]. This is not measuring RF power based on physical constants but the suggested technique may be used to compare room temperature standards with quantum standards being developed within the project [6] and which have very low output power at the moment. In this paper the measurements performed for this investigation and first results are presented. Instead of theoretical analysis experimental results are presented and a new SIC for better MW power measurements is suggested to improve accuracy and the repeatability of the technique.

2. Measurement Setup

Experimental setup is described and used instruments are given to explicitly define the experiments and these instruments are not mandatory/ advice for conducting the research.

2.1. Superconducting environment

The measurements are performed in a top loading cryo-cooler presented in [7]. The base temperature of the cooler is 2.8 K, while it can be adjusted quickly to the desired temperature via the installed heating resistors and sensors into the cooler, the temperature controller and the prepared software. A vacuum pump is used onto the top loading unit. Under vacuum, at the level of 10^{-4} mbar, superconductivity could not be observed due to the lack of temperature conduction. The temperature conduction between the cold head and the probe is established using Helium gas. The amount of Helium corresponds to the temperature conductivity of the system and is controlled via a pressure gauge. Measurements presented in the paper are performed while the pressure trough the top loading unit is around 0.1 bar. The SIC is immersed into the superconducting environment via a vacuum tight probe given in detail in [7].

2.2. Superconducting integrated circuit

The SIC used for the preliminary measurements is fabricated for JAWS [5,8] systems and has two independent arrays of JJs. There are on chip low pass filters which are used to filter high frequency impurities due to sampling and the quantization noise of the delta modulation. These filters are also optimized for wider operating margins [9]. Each array consists of coplanar waveguide (CPW) and 4000 JJs centered within the CPW. The waveguides are terminated with 50 Ω resistors to prevent the MW to reflect and disturb the stable operation of the Josephson array. The 50 Ω termination resistor is accomplished via two 100 Ω resistors arranged at the ground of the CPW. In the experiments presented in this paper, one of the arrays is used for load of MW/DC power while the other one is used as temperature sensor. The chip's layout is given in Fig.1. One of the JJs' arrays is connected to the semi rigid waveguide while the other has no waveguide connected. The critical current of the arrays is 4.5 mA.

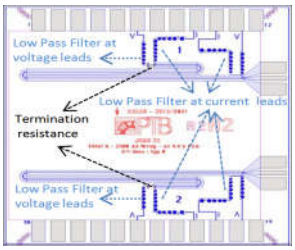

Fig.1. Chip layout and its schematics

2.3. Instrumentation setup

The critical current measurement, DC Power measurement setups and the RF source connection are all given in Fig.2. The critical current measurement principle and its equations are given in [10], the used instruments are also the same as [10]. The DC power is also applied from the same voltage source and the applied current is measured as the critical current using additional voltmeter as shown in Fig.2 by utilizing the four-wire connection onto the Josephson Junctions.

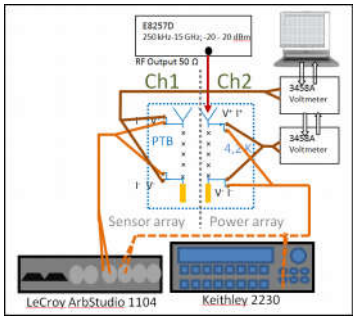

Fig.2. Instrumentation setup

2.4. Uncertainty goals versus uncertainty of the setup

The DC power on power array can be generated and measured using Equation (1). V_{JJ} is the voltage across the JJs and I_{JJ} is the current flowing through the JJs. Microwave power starting from 0 - 10 dBm (1-10 mW) is defined with an uncertainty of 4-10 mW/W in the CMCs of TÜBİTAK UME. The developed sensor will be compared with room temperature standards within this uncertainty. With this uncertainty goals the uncertainty of the setup given in Fig.2 is evaluated. Gain stability of the LeCroy sources (corresponds to stability of V_{LeCroy}) are investigated and declared in [10]: The gain stability is much less than 20 µV/V. The accuracy of the voltmeters (accuracy of V_{3458}) also are estimated to be around 20 µV/V. LeCroy source calibration combined with its stability yields uncertainty around 30 µV/V. The biggest uncertainty component is the output resistor of the Lecroy source (R_{LeCroy}) used to calculate the current. This resistor has stability of about 500 µΩ/Ω [10]. Following the calibration procedure described in [10] the total uncertainty of the output resistor of the LeCroy voltage source is estimated to be 501 µΩ/Ω. Using the Equation (1), total DC or LF power uncertainty arising from the setup is estimated 503 µW/W. Replacing (R_{LeCroy}) source by deploying additional more stable resistor and a voltmeter is also possible for future experiments.

$$P_{DC/LF}=V_{JJ}\times I_{JJ}=V_{3458}\times(V_{3458}-V_{LeCroy})/R_{LeCroy} \quad (1)$$

3. Measurements

3.1. Measuring the attenuation of the probe using conventional standards

The two identical semi rigid waveguides of the probe are shorted at the cold side of it. The attenuation of the both lines is measured from the 300 K side of the probe. The measurement is performed using RF source, RF power meter and its sensor. The output power of the high frequency source is firstly measured using the power meter and the measured power is denoted P_{in}. The same power meter is then connected to the one end of the probe while the same power settings are applied from the RF source to the other end and the power meter's reading denoted P_{out} this time. The attenuation results are plotted in Fig.3 The conventional attenuation A_{conv}, of the probe's single line is calculated using Equation (2) which is a rough estimation of the actual value.

$$A_{conv}=10.\log(P_{out}/P_{in})/2 \quad (2)$$

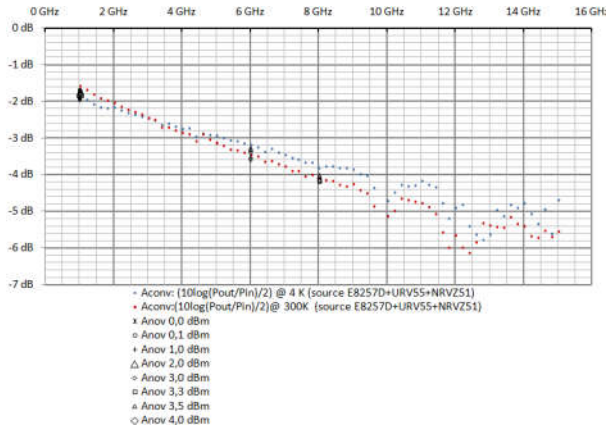

Fig.3. Average transmission of the waveguides and transmission calculated using the novel method at different power levels

3.2. Critical current measurement

There are different critical current measurement methods [4, 11]. The critical current used in the measurement is iterating the applied current and sensing voltage. The critical current measurement is the main actor of the novel method. When measured current-voltage curve is observed, it is repeatable. The nature of the AC measurement, while measuring it by comparing with DC via the temperature transfer needs quick switching between DC and AC, so the determination of the critical current should be made under software control. The first derivative of the voltage measurement versus current measurement is a good indicator of the critical current. While measuring the critical current, the temperature onto the cooler is observed. It is found that the temperature stability is affected by the critical current measurement. For this reason, the critical current measurement is interrupted immediately after the threshold of the derivative is sensed.

3.2.1. Critical current versus temperature

A certain threshold for the decision is selected by measuring critical current repeatability at different temperature settings of the cryocooler. The threshold of the derivative is selected empirically such that the critical current repeatability is better than 1 mA/A. Critical current (I_c) measurement is repeated 10

times and the type A uncertainty is declared in Table 1. Instead of set temperature of the cooler measured temperature is used for better temperature critical current dependence investigation. While there is room of improving the critical current measurements the algorithm the method and threshold is found sufficient to compare the DC power and the RF power at the goal uncertainties.

Table 1. Critical current versus temperature

Temp.	I_c	u(A) (1σ)	Temp.	I_c	u(A) (1σ)
3.093 K	11.654 mA	0.73 mA/A	3.527 K	9.621 mA	0.21 mA/A
3.093 K	11.652 mA	0.78 mA/A	3.623 K	9.010 mA	0.36 mA/A
3.189 K	11.283 mA	0.69 mA/A	3.719 K	8.420 mA	0.55 mA/A
3.285 K	10.887 mA	0.41 mA/A	4.983 K	2.536 mA	0.78 mA/A
3.430 K	10.151 mA	0.53 mA/A	4.103 K	5.998 mA	0.01 mA/A

3.2.2. Critical current versus DC power

After selecting the threshold of the derivative for the sensor array, the repeatability is measured also under DC Power applied to the neighbor power array of JJs. DC power is applied independently from the LeCroy source using additional power source seen in Fig.2 for the MW/DC power array. The DC power is applied such that the voltage onto the array is 5 times larger than the quantum voltage at 15 GHz. For the DC power values from 0.4 V to 0.9 V the critical current measurement stability still remained better than 1 mA/A (Table 2). Under 0.6 V, critical current measurement stability versus 10 times longer than the measurement in Table 2 is also investigated. Each measurements deviation from the average value is found less than 3 mA/A.

Table 2. DC Power versus critical current measurements

DC Power Source (V)	I_c (mA)	u(A) (1 σ) mA/A	DC Power Source (V)	I_c (mA)	u(A) (1 σ) mA/A
0.4	9.399	0.00	0.7	6.178	0.70
0.5	8.218	0.80	0.9	3.946	0.82
0.6	7.389	0.70			

3.2.3. Critical current & cooler temperature versus only RF power

A maximum power of 20 dBm is applied to the power array given in the setup in Fig.2. 50 mK rise in temperature of the cooler is observed due to maximum MW power. On chip temperature is found to be much higher by measuring critical current versus MW power. For this purpose, MW power at 1 GHz, is increased by 1 dBm and corresponding critical current is observed (Fig.4). 1 GHz is selected for the first investigations because the MW attenuation of the prop is less at this frequency compared to the other frequencies. This experiment is repeated several times and repeatability of the critical current is observed. The average of the measurements is fitted (the bold red equation in Fig 5.a) and measurements are compared with the mean fit and presented Fig 5. b). Measurements in Fig. 5 clearly show the critical current and microwave dependence. Nevertheless reliable and repeatable absolute curve between critical current and MW power could not be observed as can be seen from the difference of every measurement from the mean fitted curve given in Fig.4 b). Stability of the critical current at high and at low MW power is worse compared to the MW power levels between 2 mW - 7 mW as can be seen in Fig.5. Stability is also plotted dependent on the level of the critical current in Fig.6. When the MW power is low, as a consequence heating is low and the critical current is high, the stability is worse.

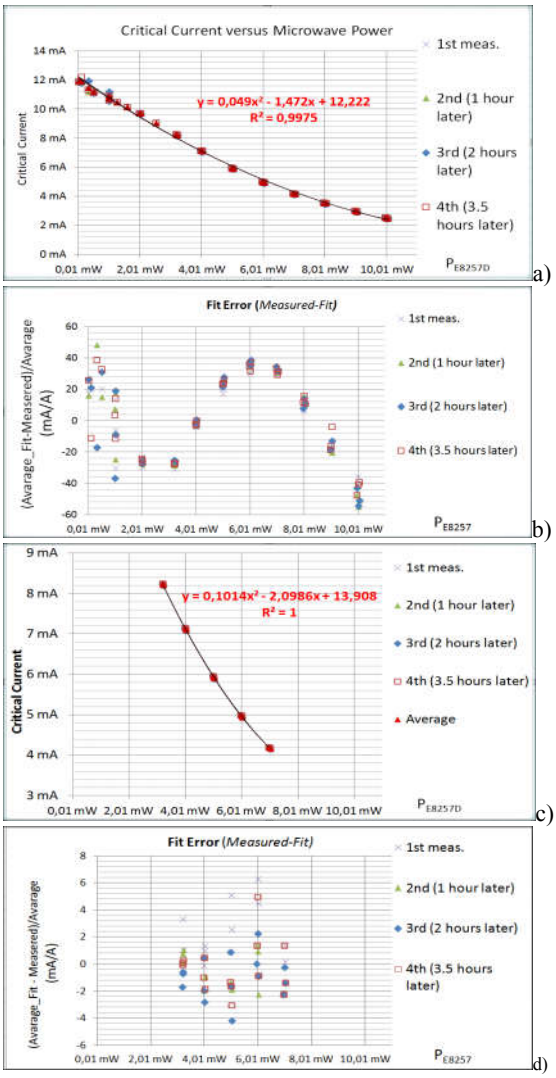

Fig.4. Critical current versus only RF Power at 1 GHz

When the critical current is low and the MW power is high the stability of the critical current measurements gets worse again. The stability of the critical current measurements is worse under MW power compared to the measurements in Table 1 and Table 2. Because of nonstable range, the analysis shown in Fig 5.a is repeated only for measurement data within the 3 mW – 7 mW range the regression coefficient is getting closer to 1 (Fig. 5c) and the fit errors are getting less and uncorrelated (Fig. 5.d). Additionally, every 1 dBm power iteration step from the MW source, is fine iterated at the ±4 mW/W of the 1 dBm power iteration, to observe if the critical current measurement is sensitive at the level of uncertainty of the MW. Measurements as in Fig.7 show that in certain region of the critical current the sensitivity of the critical current can be at the uncertainty of the MW. Similar investigations as shown in Fig.5 and Fig.6 and Fig 7 are made for MW power superimposed with DC power. The level of superimposed DC Power is chosen to be at least around 1.9 mW. The critical current measurement stability at low MW power clearly is reduced below 4 mA/A even for -20 dBm (0.01 mW). The level of superimposed DC power is increased up to 7.13 mW. The stability of critical current measurements is reduced because of the decreasing critical current level.

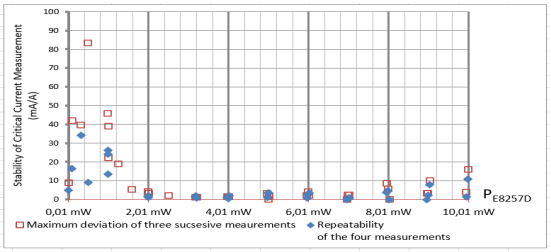

Fig.5. MW power versus critical current stability of the measurements obtained at Fig.4

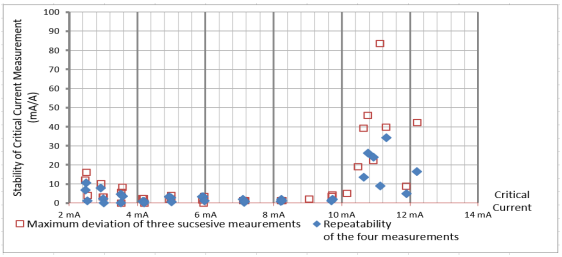

Fig.6. Critical current versus critical current stability of the measurements obtained at Fig.4

3.3. DC Power measurements

Using the second channel of the LeCroy source the current is gradually increased while the voltage is being measured simultaneously. After a target power level is reached, the current iteration is interrupted and DC Power is continuously measured. The DC Power is calculated using Equation (1). The statistics of the DC Power is also plotted on the screen under software control, and it is less than 0.1 mW/W, which is sufficient for the goal uncertainties after the DC Power is settled. Unfortunately, the desired output DC power could not be adjusted fine might be because, the curve of the DC power versus current off the JJs is not stable versus applied power level.

3.4. Absolute MW power measurement using the novel method

Measurements in Fig.4 clearly shows the critical current versus RF power dependence while its sensitivity coefficient may not have constant value over the whole MW power range and the curves may not have absolute stability. For this reason, three successive critical current measurements are performed. The first measured critical current is denoted $I_{C+DC+MW}$ and is measured under DC and MW power applied simultaneously denoted with P_{DC+MW} (P_{DC+MW} =P_{DC}+P_{MW}). The second critical current is denoted $I_{C\text{-}DCmax}$ and is measured under DC power denoted P_{DCmax} (P_{DCmax}=P_{DC+MW}+~0.5 mW) and the third critical current is denoted $I_{C\text{-}DC\text{-}min}$ and is measured under P_{DCmin} (P_{DCmin}=P_{DC+MW}-~0.5 mW). The ±~ 0.5 mW or less DC power iteration could not be accomplished easily by software, the JJs has different resistance at different power levels, as a consequence the target power couldn't be estimated under software, as a consequence the sequence of the three measurements was repeated many times by setting target DC powers benefiting from previous experimental results. The critical current measurements and corresponding DC power

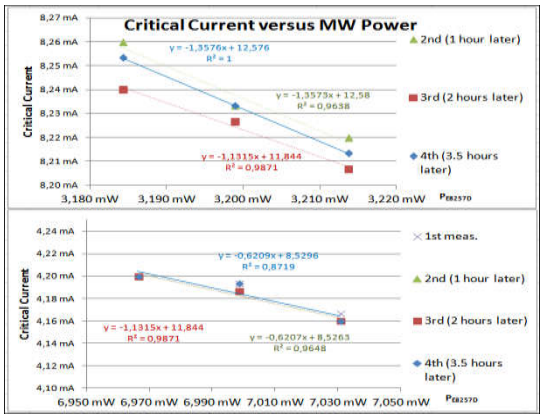

Fig.7. Critical current sensitivity versus fine adjusted MW power

measurements are performed simultaneously using a customized software. Using the DC power measurement and critical current measurement the microwave power reaching the power array is calculated using the Equation (3) and denoted P_{MW}. The three measurements are successively performed in short time in between fully automatically. An example of the raw data and P_{MW} calculated with the row data using Equation (3) is presented in Table 3.

$$P_{DC+MW}=(I_{C\text{-}DC+MW} - I_{C\text{-}DCmin})\times((P_{DCmax}-P_{DCmin})/(I_{C\text{-}DCmax}-I_{C\text{-}DCmin}))+P_{DCmin} ;$$

$$P_{MW}=P_{DC+MW}-P_{DC} \quad (3)$$

Table 3. Raw data and P_{MW} calculated using Equation (3)

P_{E8257D}=3.3 dBm(2.138 mW) @ 8 GHz							
$I_{C\text{-}DCmax}$	P_{DCmax}	$I_{C\text{-}DCmin}$	P_{DCmin}	$I_{C\text{-}DC+MW}$	P_{DC}	P_{DC+MW}	P_{MW}
3.06 mA	5.233 mW	4.38 mA	3.882 mW	3.58 mA	3.882 mW	4.701 mW	0.819 mW
3.04 mA	5.234 mW	4.42 mA	3.884 mW	3.58 mA	3.884 mW	4.706 mW	0.822 mW

3.5. Estimating the attenuation of the probe using the novel power measurement method

Conventional method described in 3.1 is more robust to the sensor calibration. Instead of measuring the output power using the power meter, which is used for testing purposes in the and is not calibrated, the output power level indicated at the source denoted PE8257D is used for attenuation calculations this time. The Equation (4) is used to calculate the attenuation A_{nov} (nov=novel) and to distinguish it from the attenuation calculated with the Equation (2). A_{nov} is used to test the novel power measurement method. For every measured P_{MW} (using Equation (3)), A_{nov} is calculated and shown in Table 4, also plotted in Fig.4 to verify the novel power measurement. Both measurements A_{conv} and A_{nov} agree on less than ±0.2 dB at every measured power level and frequency. The reason of the disagreement of ±0.2 dB might be: The probe's attenuation Aconv is roughly estimated and the two semirigid lines may not have equal attenuation, The output of MW source is not calibrated and DC Power for Anov could not be fine adjusted. Moreover any correction of MW power reflection from SIC is not performed.

$$A_{nov}=10.\log(P_{MW}/P_{E8257D}) \quad (4)$$

Table 4. Attenuation of the probe calculated with novel method

Freq.	P_{E8257D}	Anov	Freq.	P_{E8257D}	Anov	Freq.	P_{E8257D}	Anov
1 GHz	0,0 dBm	-1,9 dB	1 GHz	2,0 dBm	-1,8 dB	6 GHz	3,0 dBm	-3,6 dB
1 GHz	0,0 dBm	-1,9 dB	1 GHz	2,0 dBm	-1,8 dB	6 GHz	3,0 dBm	-3,5 dB
1 GHz	0,1 dBm	-1,7 dB	1 GHz	2,0 dBm	-1,7 dB	6 GHz	3,0 dBm	-3,4 dB
1 GHz	0,1 dBm	-1,7 dB	1 GHz	3,0 dBm	-1,9 dB	6 GHz	3,0 dBm	-3,3 dB
1 GHz	1,0 dBm	-1,7 dB	1 GHz	3,0 dBm	-2,0 dB	6 GHz	3,5 dBm	-3,3 dB
1 GHz	1,0 dBm	-1,8 dB	1 GHz	4,0 dBm	-1,8 dB	6 GHz	3,5 dBm	-3,3 dB
1 GHz	1,0 dBm	-1,7 dB	1 GHz	4,0 dBm	-1,8 dB	8 GHz	3,5 dBm	-4,0 dB
1 GHz	1,0 dBm	-1,8 dB				8 GHz	3,5 dBm	-4,0 dB
1 GHz	2,0 dBm	-1,8 dB				8 GHz	3,3 dBm	-4,2 dB

3.6. Repeatability for comparison and validation

By roughly estimating 4 mA/A critical current measurement stability and 1 mW/W DC power measurement stability, benefiting from Equation (3) and uncertainty propagation law, the stability for the novel method can be estimated to be 7 mW/W-8 mW/W (less than 0.07 dB). The maximum deviation (repeatability) of the prop attenuation presented in Table 4 at 1 GHz measurements under different power levels is 0.3 dB which is a bit larger than expected.

Measurements presented in Fig.7 show that the critical current measurement in its certain range (8 mA-3 mA, (Fig 4.c)) can be sufficiently sensitive because, the MW power is fine adjusted and critical current measurements followed this change without overlapping. Critical current can be adjusted to its sensitive range by superimposing MW power and DC Power. The fine adjustment in DC power could not be accomplished easily, as the four-wire connection is onto JJs and the resistance of JJs is temperature and power level dependent, as a consequence, the power is not predictable by the software. Instead, a resistor which has constant slope versus power on it is better for fine DC power prediction by the software. Additionally, while the DC power is imposed onto the JJs its resistance is getting high, the resistance from MW power source side is getting higher than 50 Ω and this is the reason of mismatch (reflection) errors at high frequencies. Moreover, the stability of the critical currents under only MW power is worse than its temperature dependence and DC power measurements. The termination resistors shown in Fig.1 are not within the coplanar waveguide but arranged at the ground of CPW. Even their size is too small to behave as an antenna at the frequencies the measurements are performed, this scheme reminds high frequency interference within the chip. The LeCroy source used and shown in Fig.2 has common low between all of its channels, that might make the interference worse but it is expected that the on chip low pass filters already filtered the MW power.

4. New Sensor Design

To improve the measurements new sensor design is suggested that can be accomplished quickly using the existing JAWS designs and coplanar waveguides developed for JAWS. In the new sensors one JAWS array is centered on chip, symmetrically on its both sides RF power and DC power resistors completely within the coplanar waveguide are placed with equal distances to the JAWS array. The 50 Ω DC power resistor and 50 Ω MW power resistor are both planned to be at the end of the waveguide with no JJs and with equal size and distance to the sensor JJs array. The four-wire connection to the DC power resistor is planned to be via on chip low pass filters while there is no four-wire connection to the RF power resistor.

To investigate the effect of using two separate resistors for DC and MW one additional design is suggested. The DC power resistor design is duplicated instead of MW power resistor. This time the current connection shown in Fig.1 is planned to be wired after the voltage filter, to reduce any MW interference because of the short wire.

PCB's suitable to mount and wire bond the new chips are designed, which have on PCB characteristic impedance of nearly 50 Ω for MW planned to be manufactured from Roger RT/DUROID5880.

7. Conclusion

In this paper we investigated the use of JAWS SIC consisting of two JJs arrays for microwave (MW) power measurements. The critical current was used to compare the DC power and the MW power reaching the adjacent array. Measurements were performed to develop the new measurement procedure. Validation of the method was roughly demonstrated by measuring the attenuation of the probe using the novel MW power sensor and compare it with the conventional method. The 0.2 dB consistence of the attenuation measurements between the conventional and the novel method at different power levels shows that the method can be useful for certain applications in the future. To improve the repeatability and the accuracy by automation, which is essential for such measurements, new power sensor chips were designed and will be fabricated and tested soon.

Acknowledgement

This research is partly funded within "Establishing Josephson Arbitrary Waveform Synthesizer Project" and "G2AK-E9-31-K:2017K120940-2017K12-391 UME Research Infrastructure Renovation and Development Project" of TÜBİTAK UME and partly funded with 20FUN07 SuperQuant. 20FUN07 SuperQuant has received funding from the EMPIR programme co-financed by the Participating States from the European Union‘s Horizon 2020 research and innovation programme. T.C.Ö. thanks to M.Arifoviç for his leading the resources in the lab and for the discutions on the subject.

6. References

[1] Arifovic, M., Klonz, M. "AC/DC voltage transfer at UME", Conference on Precision Electromagnetic Measurements (CPEM 2002), Ottawa (16-21/06/2002) : p

[2] Christian Donnely, Development of Quantum Based Superconducting Radio Frequency Voltage Standard" March 2019

[3] M.Schubert,M. at al."A dry-cooled Ac quantum voltmeter" Supercond. Sci.Technol. 29 (2016)15014(8pp),

[4] Paolo Durandetto, Andrea Sosso "Using a Josephson junction as an effective on-chip temperature sensor", Supercond. Sci. Technol. 34(2021) 045008,https://doi.org/10.1088/1361-6668/abdcc4

[5] Oliver F.O. Kieler, Thomas Scheller, Johannes Kohlmann "Cryocooler Operation of a Pulse-Driven AC Josephson Voltage Standard at PTB" World Journal of Condensed Matter Physics, 2013,3189-193,http://dx.doi.org/10.4236/wjcmp.2013.34031

[6] M.Bieler at al. " Microwave metrology for superconducting quantum circuits" CPEM 2022, Wellington, Nuova Zelanda

[7] Coskun Ozturk, T., at al. "Electro-optic Pulse Drive of Josephson Arbitrary Waveform Synthesizer at UME", 10th International Conference on Electrical and Electronics Engineering, İstanbul (08-10/05/2023) : 5 p.

[8] S.P. Benz, Clark A. Hamilton, "A pulse driven programmable Josephson Voltage standard" Appl. Phys. Lett.,1996,68 (3171-3173)

[9] Wattanable M., P.D. Dresselhaus, and S.P.Benz, "Resonance-free lowpass filters for the AC Josephson voltage stanard", IEEE Trans.Appl. Supercond.,2006,16, (49-53)

[10] Coskun Ozturk T., at al."Establishing Programmable Josephson Voltage Standard and Maintaining its Quantum Accuracy", International Journal of Electrical and Electronic Engineering and Telecommunications, 8:1 (2019): 19-25]

[11] Razmik A.Hovhannisyan, Olena M.Kapran, Taras Golod,Vladimir M.Krasnov,"Accurate Determination of the Josephson Critical Current by Lock-In Measurements, Nanomaterials brief report